

Jet structure of baryon excess in Au+Au collisions at $\sqrt{s_{NN}} = 200$ GeV

S. S. Adler,⁵ S. Afanasiev,²⁰ C. Aidala,^{5,10} N. N. Ajitanand,⁴⁷ Y. Akiba,^{23,42} A. Al-Jamel,³⁷ J. Alexander,⁴⁷ R. Amirkas,¹⁴ K. Aoki,²⁷ L. Aphecetche,⁴⁹ R. Armendariz,³⁷ S. H. Aronson,⁵ R. Averbeck,⁴⁸ T. C. Awes,³⁸ R. Azmoun,⁴⁸ V. Babintsev,¹⁷ A. Baldisseri,¹¹ K. N. Barish,⁶ P. D. Barnes,³⁰ B. Bassalleck,³⁶ S. Bathe,^{6,33} S. Batsouli,¹⁰ V. Baublis,⁴¹ F. Bauer,⁶ A. Bazilevsky,^{5,17,43} S. Belikov,^{19,17} Y. Berdnikov,⁴⁴ S. Bhagavatula,¹⁹ M. T. Bjornndal,¹⁰ J. G. Boissevain,³⁰ H. Borel,¹¹ S. Borenstein,²⁸ M. L. Brooks,³⁰ D. S. Brown,³⁷ N. Bruner,³⁶ D. Bucher,³³ H. Buesching,^{5,33} V. Bumazhnov,¹⁷ G. Bunce,^{5,43} J. M. Burward-Hoy,^{29,30,48} S. Butsyk,⁴⁸ X. Camard,⁴⁹ J.-S. Chai,²¹ P. Chand,⁴ W. C. Chang,² S. Chernichenko,¹⁷ C. Y. Chi,¹⁰ J. Chiba,²³ M. Chiu,¹⁰ I. J. Choi,⁵⁶ J. Choi,²² R. K. Choudhury,⁴ T. Chujo,⁵ V. Cianciolo,³⁸ Y. Cobigo,¹¹ B. A. Cole,¹⁰ M. P. Comets,³⁹ P. Constantin,¹⁹ M. Csanád,¹³ T. Csörgő,²⁴ J. P. Cussonneau,⁴⁹ D. d'Enterria,^{10,49} K. Das,¹⁴ G. David,⁵ F. Deák,¹³ H. Delagrangé,⁴⁹ A. Denisov,¹⁷ A. Deshpande,⁴³ E. J. Desmond,⁵ A. Devismes,⁴⁸ O. Dietzsch,⁴⁵ J. L. Drachenberg,¹ O. Drapier,²⁸ A. Drees,⁴⁸ K. A. Drees,⁵ R. du Rietz,³² A. Durum,¹⁷ D. Dutta,⁴ V. Dzhordzhadze,⁵⁰ Y. V. Efremenko,³⁸ K. El Chenawi,⁵³ A. Enokizono,¹⁶ H. En'yo,^{42,43} B. Espagnon,³⁹ S. Esumi,⁵² L. Ewell,⁵ D. E. Fields,^{36,43} C. Finck,⁴⁹ F. Fleuret,²⁸ S. L. Fokin,²⁶ B. D. Fox,⁴³ Z. Fraenkel,⁵⁵ J. E. Frantz,¹⁰ A. Franz,⁵ A. D. Frawley,¹⁴ Y. Fukao,^{27,42,43} S.-Y. Fung,⁶ S. Gadrat,³¹ S. Garpman,^{32,*} M. Germain,⁴⁹ T. K. Ghosh,⁵³ A. Glenn,⁵⁰ G. Gogiberidze,⁵⁰ M. Gonin,²⁸ J. Gosset,¹¹ Y. Goto,^{42,43} R. Granier de Cassagnac,²⁸ N. Grau,¹⁹ S. V. Greene,⁵³ M. Grosse Perdekamp,^{18,43} W. Guryn,⁵ H.-Å. Gustafsson,³² T. Hachiya,¹⁶ J. S. Haggerty,⁵ H. Hamagaki,⁸ A. G. Hansen,³⁰ E. P. Hartouni,²⁹ M. Harvey,⁵ K. Hasuko,⁴² R. Hayano,⁸ N. Hayashi,⁴² X. He,¹⁵ M. Heffner,²⁹ T. K. Hemmick,⁴⁸ J. M. Heuser,^{42,48} M. Hibino,⁵⁴ P. Hidas,²⁴ H. Hiejima,¹⁸ J. C. Hill,¹⁹ R. Hobbs,³⁶ W. Holzmann,⁴⁷ K. Homma,¹⁶ B. Hong,²⁵ A. Hoover,³⁷ T. Horaguchi,^{42,43,51} T. Ichihara,^{42,43} V. V. Ikonnikov,²⁶ K. Imai,^{27,42} M. Inaba,⁵² M. Inuzuka,⁸ D. Isenhower,¹ L. Isenhower,¹ M. Ishihara,⁴² M. Issah,⁴⁷ A. Isupov,²⁰ B. V. Jacak,⁴⁸ W. Y. Jang,²⁵ Y. Jeong,²² J. Jia,⁴⁸ O. Jinnouchi,^{42,43} B. M. Johnson,⁵ S. C. Johnson,²⁹ K. S. Joo,³⁴ D. Jouan,³⁹ F. Kajihara,⁸ S. Kametani,^{8,54} N. Kamihara,^{42,51} M. Kaneta,⁴³ J. H. Kang,⁵⁶ S. S. Kapoor,⁴ K. Katou,⁵⁴ T. Kawabata,⁸ A. Kazantsev,²⁶ S. Kelly,^{9,10} B. Khachaturov,⁵⁵ A. Khanzadeev,⁴¹ J. Kikuchi,⁵⁴ D. H. Kim,³⁴ D. J. Kim,⁵⁶ D. W. Kim,²² E. Kim,⁴⁶ G.-B. Kim,²⁸ H. J. Kim,⁵⁶ E. Kinney,⁹ W. W. Kinnison,³⁰ A. Kiss,¹³ E. Kistenev,⁵ A. Kiyomichi,^{42,52} K. Kiyoyama,³⁵ C. Klein-Boesing,³³ H. Kobayashi,^{42,43} L. Kochenda,⁴¹ V. Kochetkov,¹⁷ D. Koehler,³⁶ T. Kohama,¹⁶ R. Kohara,¹⁶ B. Komkov,⁴¹ M. Konno,⁵² M. Kopytine,⁴⁸ D. Korchetkov,⁶ A. Kozlov,⁵⁵ P. J. Kroon,⁵ C. H. Kuberg,^{1,30} G. J. Kunde,³⁰ K. Kurita,^{42,43} Y. Kuroki,⁵² M. J. Kweon,²⁵ Y. Kwon,⁵⁶ G. S. Kyle,³⁷ R. Lacey,⁴⁷ V. Ladygin,²⁰ J. G. Lajoie,¹⁹ Y. Le Bornec,³⁹ A. Lebedev,^{19,26} S. Leckey,⁴⁸ D. M. Lee,³⁰ S. Lee,²² M. J. Leitch,³⁰ M. A. L. Leite,¹³ X. H. Li,⁶ H. Lim,⁴⁶ A. Litvinenko,²⁰ M. X. Liu,³⁰ Y. Liu,³⁹ C. F. Maguire,⁵³ Y. I. Makdisi,⁵ A. Malakhov,²⁰ V. I. Manko,²⁶ Y. Mao,^{7,40,42} G. Martinez,⁴⁹ M. D. Marx,⁴⁸ H. Masui,⁵² F. Matathias,⁴⁸ T. Matsumoto,^{8,54} M. C. McCain,¹ P. L. McGaughey,³⁰ E. Melnikov,¹⁷ F. Messer,⁴⁸ Y. Miake,⁵² J. Milan,⁴⁷ T. E. Miller,⁵³ A. Milov,^{48,55} S. Mioduszewski,⁵ R. E. Mischke,³⁰ G. C. Mishra,¹⁵ J. T. Mitchell,⁵ A. K. Mohanty,⁴ D. P. Morrison,⁵ J. M. Moss,³⁰ F. Mühlbacher,⁴⁸ D. Mukhopadhyay,⁵⁵ M. Muniruzzaman,⁶ J. Murata,^{42,43} S. Nagamiya,²³ J. L. Nagle,^{9,10} T. Nakamura,¹⁶ B. K. Nandi,⁶ M. Nara,⁵² J. Newby,⁵⁰ P. Nilsson,³² A. S. Nyanin,²⁶ J. Nystrand,³² E. O'Brien,⁵ C. A. Ogilvie,¹⁹ H. Ohnishi,^{5,42} I. D. Ojha,^{3,53} H. Okada,^{27,42} K. Okada,^{42,43} M. Ono,⁵² V. Onuchin,¹⁷ A. Oskarsson,³² I. Otterlund,³² K. Oyama,⁸ K. Ozawa,⁸ D. Pal,⁵⁵ A. P. T. Palounek,³⁰ V. Pantuev,⁴⁸ V. S. Pantuev,⁴⁸ V. Papavassiliou,³⁷ J. Park,⁴⁶ W. J. Park,²⁵ A. Parmar,³⁶ S. F. Pate,³⁷ H. Pei,¹⁹ T. Peitzmann,³³ V. Penev,²⁰ J.-C. Peng,^{18,30} H. Pereira,¹¹ V. Peresedov,²⁰ A. Pierson,³⁶ C. Pinkenburg,⁵ R. P. Pisani,⁵ F. Plasil,³⁸ M. L. Purschke,⁵ A. K. Purwar,⁴⁸ J. Qualls,¹ J. Rak,¹⁹ I. Ravinovich,⁵⁵ K. F. Read,^{38,50} M. Reuter,⁴⁸ K. Reygers,³³ V. Riabov,^{41,44} Y. Riabov,⁴¹ G. Roche,³¹ A. Romana,²⁸ M. Rosati,¹⁹ S. Rosendahl,³² P. Rosnet,³¹ V. L. Rykov,⁴² S. S. Ryu,⁵⁶ M. E. Sadler,¹ N. Saito,^{27,42,43} T. Sakaguchi,^{8,54} M. Sakai,³⁵ S. Sakai,⁵² V. Samsonov,⁴¹ L. Sanfratello,³⁶ R. Santo,³³ H. D. Sato,^{27,42} S. Sato,^{5,52} S. Sawada,²³ Y. Schutz,⁴⁹ V. Semenov,¹⁷ R. Seto,⁶ M. R. Shaw,^{1,30} T. K. Shea,⁵ I. Shein,¹⁷ T.-A. Shibata,^{42,51} K. Shigaki,^{16,23} T. Shiina,³⁰ M. Shimomura,⁵² A. Sickles,⁴⁸ C. L. Silva,⁴⁵ D. Silvermyr,^{30,32} K. S. Sim,²⁵ J. Simon-Gillo,³⁰ C. P. Singh,³ V. Singh,³ M. Sivertz,⁵ A. Soldatov,¹⁷ R. A. Soltz,²⁹ W. E. Sondheim,³⁰ S. Sorensen,⁵⁰ S. P. Sorensen,⁵⁰ I. V. Sourikova,⁵ F. Staley,¹¹ P. W. Stankus,³⁸ E. Stenlund,³² M. Stepanov,³⁷ A. Ster,²⁴ S. P. Stoll,⁵ T. Sugitate,¹⁶ J. P. Sullivan,³⁰ S. Takagi,⁵² E. M. Takagui,⁴⁵ A. Taketani,^{42,43} M. Tamai,⁵⁴ K. H. Tanaka,²³ Y. Tanaka,³⁵ K. Tanida,⁴² M. J. Tannenbaum,⁵ A. Taranenko,⁴⁷ P. Tarján,¹² J. D. Tepe,^{1,30} T. L. Thomas,³⁶ M. Togawa,^{27,42} J. Tojo,^{27,42} H. Torii,^{27,42,43} R. S. Towell,¹ V.-N. Tram,²⁸ I. Tserruya,⁵⁵ Y. Tsuchimoto,¹⁶ H. Tsuruoka,⁵² S. K. Tuli,³ H. Tydesjö,³² N. Tyurin,¹⁷ T. J. Uam,³⁴ H. W. van Hecke,³⁰ J. Velkovska,^{5,48} M. Velkovsky,⁴⁸ V. Veszprémi,¹² L. Villatte,⁵⁰ A. A. Vinogradov,²⁶ M. A. Volkov,²⁶ E. Vznuzdaev,⁴¹ X. R. Wang,¹⁵ Y. Watanabe,^{42,43} S. N. White,⁵ N. Willis,³⁹ F. K. Wohn,¹⁹ C. L. Woody,⁵ W. Xie,⁶ Y. Yang,⁷ A. Yanovich,¹⁷ S. Yokkaichi,^{42,43} G. R. Young,³⁸ I. E. Yushmanov,²⁶ W. A. Zajc,^{10,†} C. Zhang,¹⁰ S. Zhou,⁷ S. J. Zhou,⁵⁵ J. Zimányi,²⁴ L. Zolin,²⁰ and X. Zong¹⁹

(PHENIX Collaboration)

¹Abilene Christian University, Abilene, Texas 79699, USA²Institute of Physics, Academia Sinica, Taipei 11529, Taiwan³Department of Physics, Banaras Hindu University, Varanasi 221005, India⁴Bhabha Atomic Research Centre, Bombay 400 085, India

*Deceased.

†PHENIX Spokesperson: zajc@nevis.columbia.edu

- ⁵Brookhaven National Laboratory, Upton, New York 11973-5000, USA
⁶University of California - Riverside, Riverside, California 92521, USA
⁷China Institute of Atomic Energy (CIAE), Beijing, People's Republic of China
⁸Center for Nuclear Study, Graduate School of Science, University of Tokyo, 7-3-1 Hongo, Bunkyo, Tokyo 113-0033, Japan
⁹University of Colorado, Boulder, Colorado 80309, USA
¹⁰Columbia University, New York, New York 10027 and Nevis Laboratories, Irvington, New York 10533, USA
¹¹Dapnia, CEA Saclay, F-91191, Gif-sur-Yvette, France
¹²Debrecen University, H-4010 Debrecen, Egyetem tér 1, Hungary
¹³ELTE, Eötvös Loránd University, H-1117 Budapest, Pázmány P. s. 1/A, Hungary
¹⁴Florida State University, Tallahassee, Florida 32306, USA
¹⁵Georgia State University, Atlanta, Georgia 30303, USA
¹⁶Hiroshima University, Kagamiyama, Higashi-Hiroshima 739-8526, Japan
¹⁷Institute for High Energy Physics (IHEP), Protvino, Russia
¹⁸University of Illinois at Urbana-Champaign, Urbana, Illinois 61801, USA
¹⁹Iowa State University, Ames, Iowa 50011, USA
²⁰Joint Institute for Nuclear Research, RU-141980 Dubna, Moscow Region, Russia
²¹KAERI, Cyclotron Application Laboratory, Seoul, Korea
²²Kangnung National University, Kangnung 210-702, Korea
²³KEK, High Energy Accelerator Research Organization, Tsukuba-shi, Ibaraki-ken 305-0801, Japan
²⁴KFKI Research Institute for Particle and Nuclear Physics (RMKI), H-1525 Budapest 114, P.O. Box 49, Hungary
²⁵Korea University, Seoul, 136-701, Korea
²⁶Russian Research Center "Kurchatov Institute," Moscow, Russia
²⁷Kyoto University, Kyoto 606, Japan
²⁸Laboratoire Leprince-Ringuet, Ecole Polytechnique, CNRS-IN2P3, Route de Saclay, F-91128, Palaiseau, France
²⁹Lawrence Livermore National Laboratory, Livermore, California 94550, USA
³⁰Los Alamos National Laboratory, Los Alamos, New Mexico 87545, USA
³¹LPC, Université Blaise Pascal, CNRS-IN2P3, Clermont-Fd, F-63177 Aubiere Cedex, France
³²Department of Physics, Lund University, Box 118, SE-221 00 Lund, Sweden
³³Institut für Kernphysik, University of Muenster, D-48149 Muenster, Germany
³⁴Myongji University, Yongin, Kyonggido 449-728, Korea
³⁵Nagasaki Institute of Applied Science, Nagasaki-shi, Nagasaki 851-0193, Japan
³⁶University of New Mexico, Albuquerque, New Mexico 87131, USA
³⁷New Mexico State University, Las Cruces, New Mexico 88003, USA
³⁸Oak Ridge National Laboratory, Oak Ridge, Tennessee 37831, USA
³⁹IPN-Orsay, Université Paris Sud, CNRS-IN2P3, BP1, F-91406, Orsay, France
⁴⁰Peking University, Beijing, People's Republic of China
⁴¹PNPI, Petersburg Nuclear Physics Institute, Gatchina, Russia
⁴²RIKEN (The Institute of Physical and Chemical Research), Wako, Saitama 351-0198, Japan
⁴³RIKEN BNL Research Center, Brookhaven National Laboratory, Upton, New York 11973-5000, USA
⁴⁴St. Petersburg State Technical University, St. Petersburg, Russia
⁴⁵Universidade de São Paulo, Instituto de Física, Caixa Postal 66318, São Paulo CEP05315-970, Brazil
⁴⁶System Electronics Laboratory, Seoul National University, Seoul, Korea
⁴⁷Chemistry Department, Stony Brook University, Stony Brook, SUNY, New York 11794-3400, USA
⁴⁸Department of Physics and Astronomy, Stony Brook University, SUNY, Stony Brook, New York 11794, USA
⁴⁹SUBATECH (Ecole des Mines de Nantes, CNRS-IN2P3, Université de Nantes) BP 20722 - 44307, Nantes, France
⁵⁰University of Tennessee, Knoxville, Tennessee 37996, USA
⁵¹Department of Physics, Tokyo Institute of Technology, Tokyo, 152-8551, Japan
⁵²Institute of Physics, University of Tsukuba, Tsukuba, Ibaraki 305, Japan
⁵³Vanderbilt University, Nashville, Tennessee 37235, USA
⁵⁴Waseda University, Advanced Research Institute for Science and Engineering, 17 Kikui-cho, Shinjuku-ku, Tokyo 162-0044, Japan
⁵⁵Weizmann Institute, Rehovot 76100, Israel
⁵⁶Yonsei University, IPAP, Seoul 120-749, Korea

(Received 7 August 2004; published 27 May 2005)

Two particle correlations between identified meson and baryon trigger particles with $2.5 < p_T < 4.0$ GeV/ c and lower p_T charged hadrons have been measured at midrapidity by the PHENIX experiment at RHIC in $p+p$, $d+Au$, and $Au+Au$ collisions at $\sqrt{s_{NN}} = 200$ GeV. In noncentral $Au+Au$ collisions, the probability of finding a hadron near in azimuthal angle to the trigger particles is almost identical for mesons and baryons and significantly higher than in $p+p$ collisions. The associated yields for trigger baryons decrease in the most central collisions, consistent with some baryon production by thermal recombination in addition to hard scattering.

A remarkable feature of relativistic heavy ion collisions is greatly enhanced production of baryons and antibaryons relative to mesons. This enhancement over elementary $p+p$ collisions occurs at transverse momenta (p_T) of 2–5 GeV/ c [1–3]. In this range, particle production shifts from soft processes (nonperturbative, low momentum transfer scattering) to hard (high momentum transfer parton-parton scattering). Hard scattering is followed by fragmentation of the scattered partons to jets of hadrons. Baryon and antibaryon production is suppressed in fragmentation in vacuum. Phenomenologically, this can be thought of as a large penalty for creating a diquark/antidiquark pair for baryons vs. a quark/antiquark pair for meson formation.

Since there is no sharp separation of scales between hard and soft processes, it is natural to ask which causes the baryon excess in Au+Au collisions. Hadron formation by coalescence of quarks from the expanding thermal fireball can explain single particle yields [4–7] but causes no jetlike correlations. The yield of baryons in this momentum range scales approximately with the number of binary nucleon-nucleon collisions [2], which is typical of hard processes. However, if hard scattering is at the root of the baryon excess, additional mechanisms absent in elementary $p+p$ collisions are required, such as alteration of the jet fragmentation function in the dense medium formed in Au+Au collisions, or recombination of hard scattered quarks with accidental comoving quarks from the medium. Models include hard parton fragmentation but recombination of thermal quarks only [5], thermal quark recombination with jet fragments [6,8], and recombination of quarks from hard scattering with a modified fireball distribution [7]. Hadron production via recombination between jet fragments and thermal quarks [6–8] could preserve jetlike correlations among the final hadrons, presuming that each hadron contains at least one quark arising from a fragmenting hard scattered parton.

To determine the role of jets in production of intermediate p_T protons, the PHENIX experiment at RHIC has measured energetic hadronic partners near the baryons. These are the additional fragmentation products from the same jet as the baryon. We present first results on two particle correlations where the *trigger* particle is an identified meson (π , K) or baryon (p , \bar{p}) at $2.5 < p_T < 4.0$ GeV/ c . *Associated* particles, i.e., lower p_T charged hadrons near the trigger particle in azimuthal angle are counted. A Monte Carlo study shows that for these trigger particle momenta, resonance decays do not contribute associated particles at $p_T > 1.2$ GeV/ c ; at lower p_T , there is a small contribution, but it is less than the statistical uncertainty. The centrality and collision system dependence of the associated particle yield per trigger is measured. Trigger particles from recombination of boosted thermal quarks only should not have correlated partners beyond effects of elliptic flow, as a thermal source is by definition uncorrelated. However, trigger particles from hard scattered partons should have jetlike partners with a probability depending upon the medium effect on fragmentation. We use $p+p$ collisions without trigger identification to provide a comparison baseline.

Collisions at $\sqrt{s_{NN}} = 200$ GeV of Au+Au (24 million events), $d+Au$ (42 million events), and $p+p$ (23 million

events) are analyzed. Charged particles are reconstructed in the central arms of PHENIX using drift chambers, each with azimuthal coverage of $\pi/2$, and two layers of multiwire proportional chambers with pad readout (PC1, PC3) [9]. Pattern recognition is based on a combinatorial Hough transform in the track bend plane, with the polar angle determined by PC1 and the collision vertex along the beam direction [1]. Particle momenta are measured with a resolution $\delta p/p = 0.7\% \oplus 1.0(1.1)\% p(\text{GeV}/c)$ in Au+Au ($d+Au$, $p+p$). The portion of the east arm spectrometer containing the high resolution time-of-flight (TOF) detector, which covers pseudorapidity $|\eta| < 0.35$ and $\phi = \pi/4$ in azimuthal angle, is used for trigger particle identification. Beam counters (BBC) [9] provide the global start; stop signals are from TOF scintillators at a radial distance of 5.06 m. The timing resolution is $\sigma = 120$ ps, which allows a 4σ separation of mesons/baryons up to $p_T \approx 4$ GeV/ c . The Au+Au centrality determination is described in Ref. [10].

Distributions of azimuthal angular difference $\Delta\phi$ are constructed for trigger-partner pairs. The combinatorial background is determined by constructing mixed events in two steps: the number of trigger and partner particles per event is determined by sampling the measured particle multiplicity distributions in the relevant momentum and centrality ranges. The measured trigger and partner particle momentum distributions are then sampled to yield three-momenta of particles in each mixed event. To correct for the limited acceptance of PHENIX, the real event $\Delta\phi$ distributions are divided by $\Delta\phi$ distributions from mixed events, with the integral fixed to correspond to perfect acceptance as a function of $\Delta\phi$. The shape of this distribution corrects for the $\Delta\phi$ dependence of the PHENIX azimuthal acceptance, but has no true correlations. The $\Delta\phi$ distributions are shown in Fig. 1; mixed events are indicated by solid lines. The partner yield is corrected for the reconstruction efficiency, detector aperture, and (for Au+Au only) detector occupancy [11]. No extrapolation is made to $|\eta| > 0.35$. No correction for the PHENIX $\Delta\eta$ acceptance is needed in Figs. 1 and 2, as the same acceptance is used for both trigger type and the different collision systems. Since $d+Au$ and Au+Au collisions contain uncorrelated combinatorial background from other particles in the underlying event, the mixed event partner yield per trigger, after the same efficiency correction, is subtracted. The absolute normalization of the background is obtained independently by a convolution of the trigger and partner single particle rates.

In real events, collisions from the more central edge of the bin contribute more pairs than those from the less central edge. Mixed events are constructed by randomly sampling single particle multiplicity distributions within a 5% centrality bin. As the particle multiplicity is not flat with centrality, mixed events underweight the upper edge of the bin compared to real events. The mixed event background is corrected for this effect. The spread of trigger and partner number within a bin is determined from the measured centrality dependence of particle multiplicity in the relevant momentum region and particle species [10–13]. The correction modifies the background level by $\approx 0.2\%$ in the most central and $\approx 25\%$ in the most peripheral Au+Au collisions.

Elliptic flow causes an angular correlation in Au+Au unrelated to jet fragmentation, and is a background to this

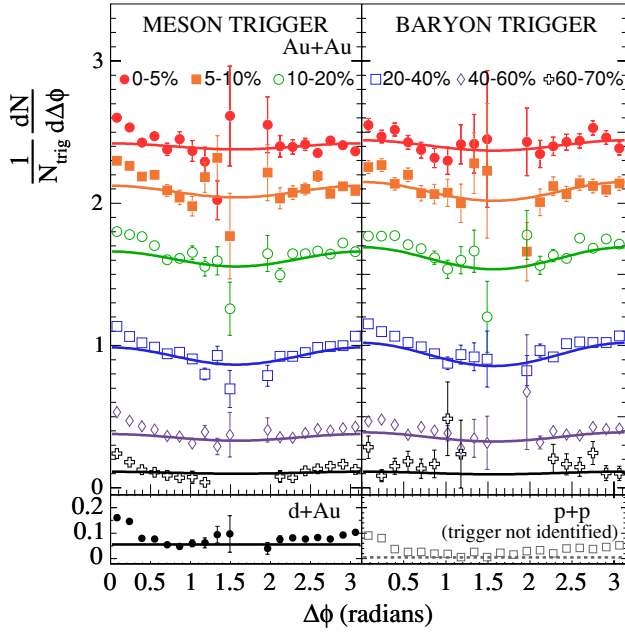


FIG. 1. (Color online) Top panels show $\Delta\phi$ distributions for meson (left) and baryon (right) triggers with $2.5 < p_T < 4.0$ GeV/ c and associated charged hadrons with $1.7 < p_T < 2.5$ GeV/ c in Au+Au collisions. Bottom panels show the same quantity for meson triggers in d +Au collisions (left) and unidentified triggers in p + p collisions (right). Lines indicate the calculated combinatorial background in the event modulated by the measured elliptic flow (Au+Au only).

measurement. The elliptic flow correlation is removed by modulating the azimuthally uniform combinatorial background by $1 + 2v_2^{\text{assoc}} v_2^{\text{trig}} \cos(\Delta\phi)$, where v_2^{assoc} and v_2^{trig} are the v_2 values measured for the partner and trigger p_T ranges, respectively [14]. The reaction plane is measured by the BBC at $3 < |\eta| < 4$ in order to minimize the influence of jets in the v_2 values. Because the centrality binning in this analysis is finer than in [14], the p_T integrated centrality dependence is used to interpolate v_2 for collisions more central than 20%. The modulation of the mixed event $\Delta\phi$ distributions is visible in Fig. 1.

Systematic uncertainties in Au+Au and d +Au partner yields arise from uncertainties in the corrections for centrality bin width, systematic and statistical errors on v_2 [14] (Au+Au only), uncertainty in the background subtraction due to the event mixing technique, and uncertainty in the detector occupancy correction. Cross-contamination of mesons and protons is less than 5%. The error on the occupancy correction reaches a maximum of 5% in the most central Au+Au collisions. For most Au+Au bins, the dominant systematic uncertainty on the partner yields is the uncertainty in v_2 . This produces a systematic error of approximately 0.01 partners per trigger baryon in semicentral and central collisions; for trigger mesons, the corresponding error is 60% of this. The event mixing uncertainty is nearly comparable. In peripheral Au+Au collisions, the dominant systematic error is from uncertainty on centrality bias corrections and v_2 . In d +Au collisions, there is no v_2 , and the partner yield uncertainty is driven by the

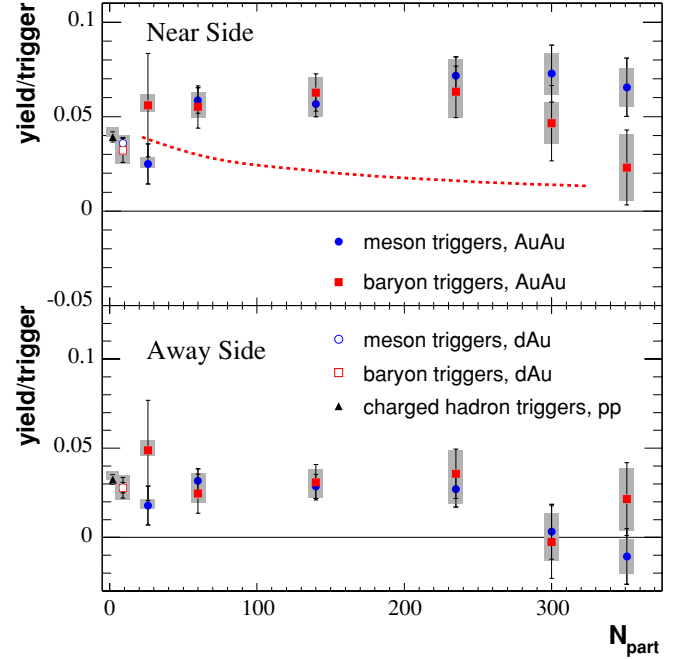


FIG. 2. (Color online) Yield per trigger for associated charged hadrons between $1.7 < p_T < 2.5$ GeV/ c for the near- (top) and away- (bottom) side jets. The error bars are statistical errors, and the gray boxes are centrality-dependent systematic errors. There is an additional 12% error on the overall normalization, which moves all points together. The dashed line (top) represents an upper limit of the centrality dependence of the near-side partner yield from thermal recombination (see text).

correction for centrality bias. In p + p collisions, the systematic error is taken to be the same size as the combinatorial background, which is subtracted. The total systematic errors are shown in Fig. 2.

The background shown in Fig. 1 is subtracted from the data points, which in most cases lie systematically above the line. The number of associated partners per trigger is integrated to determine the conditional yield of partners. The near- (far-) side yield is the integral over $0 < \Delta\phi < 0.94$ radians ($2.2 < \Delta\phi < \pi$ radians). This range maximizes the partner acceptance while omitting the region around $\Delta\phi = \pi/2$, where the TOF coverage creates an acceptance hole. Nonbackground associated partners are observed in the angular range characteristic of jet fragmentation in p + p , which was measured by PHENIX to be ≈ 0.25 radians in a similar p_T range [15].

Figure 2 shows the conditional yield per trigger of partner particles in p + p , d +Au, and Au+Au collisions, as a function of the number of participant nucleons. Small relative angle yields, from the same jet as the trigger hadron, are in the top panel. The partners increase for both trigger baryons and mesons by almost a factor of two from d +Au to peripheral and midcentral Au+Au. There is an indication that jetlike correlations for baryons relative to mesons decrease in the most central collisions, as expected for production of a fraction of the baryons by recombination of thermal quarks. It is notable, however, that the baryon excess

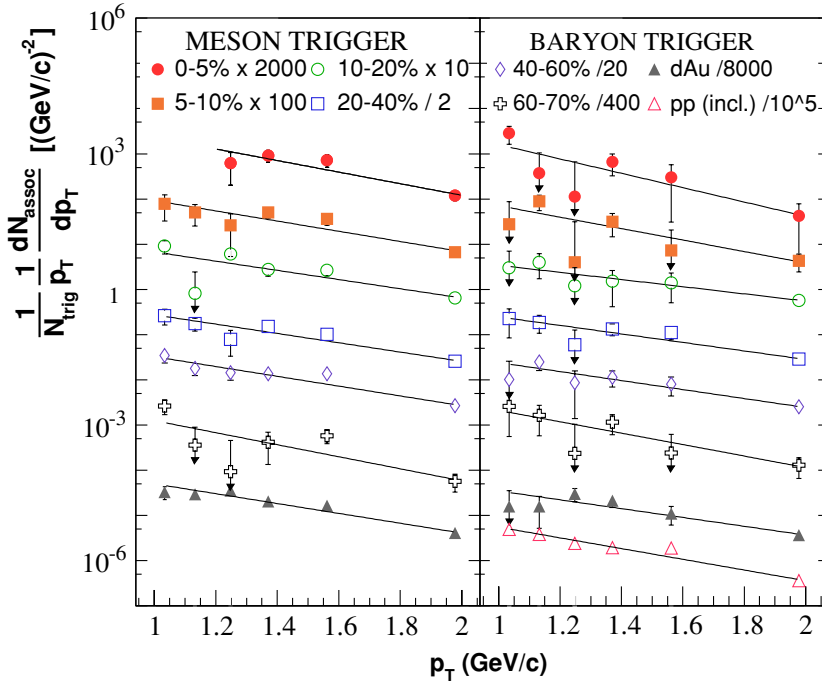


FIG. 3. (Color online) p_T spectra of the near-side associated charged hadrons corrected to the full jet yield for meson (left) and baryon (right) triggers at $2.5 < p_T < 4.0$ GeV/c and $|\eta| < 0.35$. Errors are statistical only. The curves are exponential fits.

observed via p/π ratios [1–3] is already large in mid-central collisions. In $d+Au$ collisions, the near-side yields per trigger are the same for meson and baryon triggers, and they agree with results from $p+p$ collisions generated with PYTHIA [16].

The dashed line in Fig. 2 shows the expected centrality dependence of partners per baryon if all the “extra” baryons [10], that increase p/π over that in $p+p$ collisions, were to arise solely from soft processes; such baryons dilute the per-trigger conditional yield. Because this simple estimate omits meson production by recombination, which must also occur along with baryon production, it represents an upper limit to the centrality dependence of the jet partner yield from thermal recombination. The data clearly disagree with this estimate, indicating that hard processes must also contribute to the baryon excess. The bottom panel of Fig. 2 shows the conditional yield of partners on the away side. The partner yield in $2.2 < \Delta\phi < \pi$ radians drops equally for both trigger

baryons and mesons from $p+p$ and $d+Au$ to central Au+Au, in agreement with the observed disappearance [17] and/or broadening [15] of the away-side jet. It further supports the conclusion that the baryons originate from the same jetlike mechanism as mesons.

Figure 3 shows the p_T spectra of associated particles [18] on the near side with trigger mesons and baryons. The measured transverse momentum of jet hadrons with respect to the initial parton direction $\langle j_T \rangle$ is constant as a function of collision energy and p_T [15,19]. Thus, the angular size of jets increases as the partner p_T decreases. We use the PHENIX measurement of $\langle |j_{T,y}| \rangle = 0.359 \pm 0.011$ GeV/c [15] to correct the near-side conditional yield measured in $\Delta\phi < 0.94$ radians, and the PHENIX η acceptance to the full jet yield, assuming that jets are symmetric gaussians in both ϕ and η . The conditional yields in Fig. 2 do not have this additional correction as they are measured in a single p_T bin. The partner spectra in Fig. 3 are fitted with exponentials, and the inverse slopes are given in Fig. 4. The systematic uncertainty on the associated

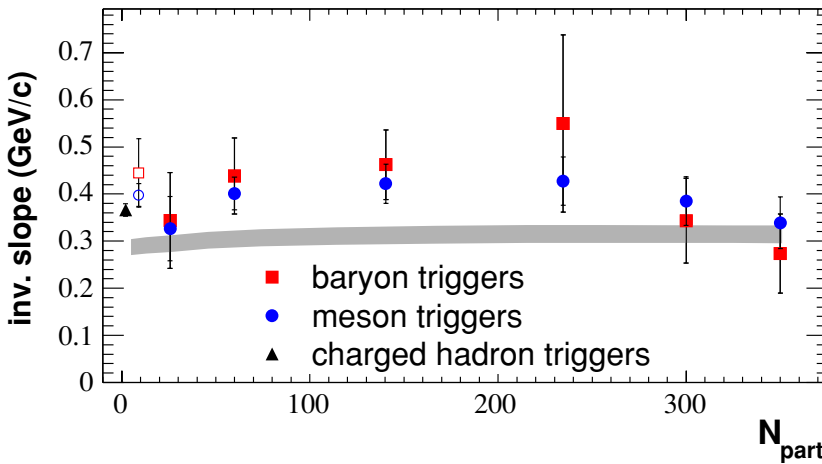


FIG. 4. (Color online) Inverse slopes from the fits in Fig. 3. Solid (open) squares and circles are Au+Au ($d+Au$), collisions and the triangle is $p+p$ collisions. The solid band indicates the slopes of inclusive particle spectra in Au+Au collisions [11]. Errors are statistical only.

particle slope in central collisions is approximately 20%, based on a conservative estimate of 50% uncertainty on the correction to the full jet yield. We note that this is comparable to the statistical error for leading mesons and smaller than the statistical error for leading baryons. Within the available statistics, the inverse slopes of the associated particles are similar for trigger mesons and baryons in $p+p$, $d+Au$, peripheral, and midcentral Au+Au. The spectra are harder than inclusive hadron spectra, as expected from jet fragmentation. In the most central Au+Au collisions, the partner and inclusive hadron spectra are in better agreement.

We have presented the first study of the jet structure of baryons (p, \bar{p}) and mesons (π, K) in the momentum region where baryon production is greatly enhanced in central Au+Au collisions at RHIC. Three observations indicate that mesons and baryons arise from hard processes in all but the most central Au+Au collisions. First, baryons and mesons both have jetlike partner particles. Second, within the limited statistics available, the inverse slopes of the associated particles are similar for both baryons and mesons; these are larger than for inclusive hadrons. Finally, on the away side, the jet partner yield into a 0.94 radian opening angle has the same centrality dependence for trigger baryons and mesons, consistent with attenuation in central collisions. The increase in jetlike partners between $p+p$ and Au+Au is strong evidence for medium modification of the fragmentation process. Recombination of thermal quarks with jet fragments [6,8] and a “wake effect” from comoving radiated gluons [7] are two examples of how the medium might modify jet fragmentation. The decrease with centrality of partner yields for trigger baryons suggests a growing contribution of baryons from thermal recombination.

We thank the staff of the Collider-Accelerator and Physics Departments at Brookhaven National Laboratory, and the staff of the other PHENIX participating institutions, for their vital contributions. We acknowledge support from the Department of Energy; the Office of Science, Nuclear Physics Division, the National Science Foundation; Abilene Christian University Research Council; the Research Foundation of SUNY; the Dean of the College of Arts and Sciences, Vanderbilt University; the Ministry of Education, Culture, Sports, Science, and Technology, and the Japan Society for the Promotion of Science (Japan); Conselho Nacional de Desenvolvimento Científico e Tecnológico and Fundação de Amparo à Pesquisa do Estado de São Paulo (Brazil); the Natural Science Foundation of China (People’s Republic of China); Centre National de la Recherche Scientifique, Commissariat à l’Énergie Atomique, Institut National de Physique Nucléaire et de Physique des Particules, and Institut National de Physique Nucléaire et de Physique des Particules (France); Bundesministerium für Bildung und Forschung, Deutscher Akademischer Austausch Dienst, and Alexander von Humboldt Stiftung (Germany); the Hungarian National Science Fund, OTKA (Hungary); the Department of Atomic Energy and Department of Science and Technology (India); the Israel Science Foundation (Israel); the Korea Research Foundation and Center for High Energy Physics (Korea); the Russian Ministry of Industry, Science and Technologies, Russian Academy of Science, Russian Ministry of Atomic Energy (Russia); VR and the Wallenberg Foundation (Sweden); the U.S. Civilian Research and Development Foundation for the Independent States of the Former Soviet Union; the US-Hungarian NSF-OTKA-MTA; the US-Israel Binational Science Foundation; and the 5th European Union TMR Marie-Curie Program.

-
- [1] K. Adcox *et al.* (PHENIX Collaboration), Phys. Rev. Lett. **88**, 022301 (2002).
 [2] S. S. Adler *et al.* (PHENIX Collaboration), Phys. Rev. Lett. **91**, 172301 (2003).
 [3] J. Adams *et al.* (STAR Collaboration), Phys. Rev. Lett. **92**, 052302 (2004).
 [4] R. C. Hwa and C. B. Yang, Phys. Rev. C **67**, 034902 (2003).
 [5] R. J. Fries, B. Muller, C. Nonaka, and S. A. Bass, Phys. Rev. Lett. **90**, 202303 (2003); Phys. Rev. C **68**, 044902 (2003).
 [6] V. Greco, C. M. Ko, and P. Levai, Phys. Rev. Lett. **90**, 202302 (2003); Phys. Rev. C **68**, 034904 (2003).
 [7] R. J. Fries, S. A. Bass, and B. Muller, Phys. Rev. Lett. **94**, 122301 (2005).
 [8] R. C. Hwa and C. B. Yang, Phys. Rev. C **70**, 024905 (2004); J. Phys. G **30**, S1117 (2004).
 [9] K. Adcox *et al.* (PHENIX Collaboration), Nucl. Instrum. Methods **A499**, 469 (2003).
 [10] S. S. Adler *et al.* (PHENIX Collaboration), Phys. Rev. C **69**, 034909 (2004).
 [11] S. S. Adler *et al.* (PHENIX Collaboration), Phys. Rev. C **69**, 034910 (2004).
 [12] C. Klein-Bösing (PHENIX Collaboration), J. Phys. G **30**, S975 (2004).
 [13] F. Matathias (PHENIX Collaboration), J. Phys. G **30**, S1113 (2004).
 [14] S. S. Adler *et al.* (PHENIX Collaboration), Phys. Rev. Lett. **91**, 182301 (2003).
 [15] J. Rak (PHENIX Collaboration), J. Phys. G **30**, S1309 (2004).
 [16] T. Sjöstrand *et al.*, Comput. Phys. Commun. **135**, 238 (2001).
 [17] C. Adler *et al.* (STAR Collaboration), Phys. Rev. Lett. **90**, 082302 (2003).
 [18] F. Wang (STAR Collaboration), J. Phys. G **30**, S1299 (2004).
 [19] A. L. S. Angelis *et al.* (CCOR Collaboration), Phys. Lett. **B97**, 163 (1980).